Dicle University
Journal of Engineering
https://dergipark.org.tr/tr/pub/dumf
duje.dicle.edu.tr

Research Article

Temperature Prediction of Lithium-ion Battery by CPSO-UKF

Göksu TAŞ[1*]

[1] Manisa Celal Bayar University, Mechatronics Engineering Department, goksu.tas@cbu.edu.tr, Orcid No: 0000-0003-2343-9182

ARTICLE INFO

Article history:

Received 5 August 2024
Received in revised form 16 September 2024
Accepted 30 September 2024
Available online 23 December 2024

Keywords:

Electric Vehicle, Lithium-ion, Temperature Prediction, Unscented Kalman Filter, Chaos Particle Swarm Algorithm

Doi: 10.24012/dumf.1528158

* Corresponding author

ABSTRACT

In this study, the temperature estimation of lithium-ion batteries is proposed by the Chaos Particle Swarm Algorithm-Unscented Kalman Filter (UKF). 18650-type lithium-ion batteries are widely used in electric vehicles due to their compact design and long life. The accurate estimation of the temperature parameter of these batteries is critical for reasons such as balancing the performance and predicting chemical degradation. Therefore, in this study, the temperature parameter estimation of an 18650-type lithium-ion battery is made by UKF-based methods. Due to the intensive and mathematical processing load of the UKF method, the parameter values are determined by Chaos Particle Swarm Optimization (PSO) methods, and their estimation performances are compared. The parameter values such as alpha, kappa, and R matrix of the UKF method are determined by Particle Swarm Optimization (PSO), Chaos Particle Swarm Optimization (CPSO), Comprehensive Learning Particle Swarm Optimization (CLPSO), and hyperparameter values determined by trial and error. The hyperparameter values obtained from these four different methods were applied to the UKF method separately, and their estimation performances were compared. The CPSO-UKF method became the most successful method by reaching an accuracy of 99.99228% in estimation according to the R^2 metric. The success of the proposed method is also given with other regression metrics.

Introduction

Due to its many benefits, including high energy density, power density, extended service life, lack of memory effect, and others, lithium-ion batteries have been widely used in new energy vehicles and portable electronics since the 1990s [1]. Recent years have seen a fast development of lithium (Li)-based metal batteries, such as Li-ion batteries, Li-S batteries, and Li-air batteries, due to the expanding uses of portable devices, electric cars, and smart grids. Power Li batteries must have high energy density in order to extend the operating mileage of applications like electric automobiles [2]. Despite its many benefits, consumers firmly believe that better lithium-ion batteries will eventually be produced since the current generation of these batteries is unable to fully meet business demands. In the realm of new energy vehicles, an optimal battery should possess not only exceptional cycle performance, high-rate capabilities, and a broad operating temperature range, but also exceptional safety performance [3]. To create batteries that are more affordable, denser, lighter, more powerful, and have a larger storage capacity, battery producers are always experimenting with novel chemistries. Presently, LIB technology has the best energy density among all innovative storage methods. For this reason, due to the many beneficial features of lithium-ion batteries, their use is critical for areas such as energy and production. It's remarkable how characteristics like quick charging and a temperature operating window between −50 °C and 125 °C can be fine-tuned thanks to the huge range of cell designs and chemicals. Other advantages of Li-ion batteries are their low self-discharge rate, lengthy lifespan, and high cycling performance, they can often withstand hundreds of charging and discharging cycles [4]. The usual temperature range of 20 to 60 °C is sufficient for lithium-ion batteries (LIBs) to store energy and function efficiently; however, below zero, performance drastically decreases [5]. Even at -40 °C, the most frost-resistant batteries continue to function, although their capacity drops to around 12%. Moreover, cycling at low temperatures speeds up LIB aging, which makes long-term battery use in cold climates restricted [6].

In addition to EVs, LIBs are widely used in a variety of portable consumer electronics products and energy storage facilities. However, cold temperatures significantly impair LIBs' functioning. The discharge capacity of LIBs rapidly decreases below 0°C, and they are unable to fulfill the low-temperature standards necessary for electronic gadgets and electric vehicles to operate normally. A study. found that at temperatures below -10°C, LIBs lose the most energy

and capacity [7]. The parameters of lithium-ion batteries are very important for the safe use of batteries under different temperature conditions. Since the temperature parameters of lithium-ion batteries cannot be determined reliably and healthily, critical problems such as incorrect prediction of battery life and energy management arise. Estimation methods for lithium-ion battery parameters are similar. For this reason, many studies have been conducted in the literature on this issue. For real-world Battery Management System (BMS) [8], [9] applications, it was presented a particle filter-based co-estimation approach for state of charge (SOC) [10] and state of heath (SOH) [11] based on the mathematically complicated P2D model, which has a time-delayed response [12]. A chaotic firefly-particle filtering technique was developed, which mimics the way in which fireflies naturally interact with one another by using light to achieve particle optimization. In order to perform high-precision SOC and SOH co-estimations, it discovers a new optimal solution by chaotically mapping a set of particles to distinct solution spaces [13]. For the purpose of co-estimating the SOC and SOH of lithium-ion batteries, a study was given that suggested a backpropagation neural network-dual extended Kalman filter (DEKF) technique based on the limited memory recursive least squares (LMRLS) algorithm. By accounting for the coupling impact between SOC and SOH, the backpropagation neural network is utilized to perform synergistic estimation, which enhances the tracking accuracy of the DEKF technique [14]. An adaptive extended H-infinity filtering approach using a particle swarm optimization network was reported in a study. This method creatively makes use of the monitoring of the battery's aging characteristics in terms of capacity and power fading for SOC and SOH estimates [15].

Since lithium-based batteries have an important place today, their importance is increasing in the future due to more consistent use of energy. As a result of the literature research, together with the importance of the above-mentioned issue and the problems that arise, it has been concluded that the temperature estimation of lithium-ion batteries is very important. In addition, it has been concluded that this problem has not been solved while determining the hyperparameter values of the UKF method with trial-and-error methods while determining the parameters of lithium-based batteries. For this reason, in this study, a solution has been provided to this problem by determining the hyperparameter values with the PSO, CPSO, and CLPSO methods in the UKF method while estimating the parameters of 18650-type lithium-ion batteries. In this study, the temperature parameter estimation performances of the PSO-UKF, CPSO-UKF, and CLPSO-UKF methods of the 18650-type lithium-ion battery have been compared and presented. The hyperparameter values of the UKF method have been determined successfully with all optimization methods, and it has yielded more successful results than the traditional UKF. The obtained results have been presented with many graphics and regression estimation metrics that can be applied in real life.

Material and Method

In this study, the dataset was edited using the MATLAB program. The obtained edited dataset was used to estimate temperature using the Python programming language on a computer running the Ubuntu operating system. The necessary codes for optimization and filtering were edited, and the results were recorded.

Experimental Data

The battery data used in this study was taken from another study published in 2023 [16]. In the experimental study conducted in the related study, a total of 25 LIBs were used for the test. 5 cells were tested for each SOH condition. An RPT was performed on each LIB when aged to 100%, 95%, 90%, 85%, and 80% SOH values through electrical cycling. To measure the retained energy capacity, the LIBs were stored in a thermal chamber at 25 °C. They were left for one hour to equilibrate. Then, each LIB was charged to 4.2 V using the C/3 constant current profile, at which point the LIB was held at this voltage and charged in constant voltage (CV) mode until the value of the charge current decreased to C/20. SOH is defined as the ratio of the cell's measured energy capacity at a particular cycle number to its measured energy capacity at the time of its first measurement. The energy capacity of the cell as measured at a specific number of cycles is expressed by its current capacity. In the relevant dataset, 90% SOH means that the battery capacity maintains 90% of its original capacity after certain cycles. For this reason, although there is no fixed cycle number for each SOH level, when the dataset is examined, it is seen that the SOH value is 90.80% in 120 cycles and 95.06% in 60 cycle numbers for a battery cell. The relevant SOH formula is given in Equation 1 [16]. Current

$$SOH = \frac{Current\ Capacity}{Reference\ Capacity} \text{ x } 100 \quad (1)$$

The characteristics of the battery used in this study are given in Table 1 [17].

Table 1. Lithium-ion battery specifications

Parameter	Details
Nominal Voltage	3.63 V
Standard Charge	Constant current 0.3C (1,455mA)
	Constant voltage 4.2V
	End current (Cut off) 50mA
Weight	68.0 ± 1.0 g
Energy	Nominal 18.20Wh

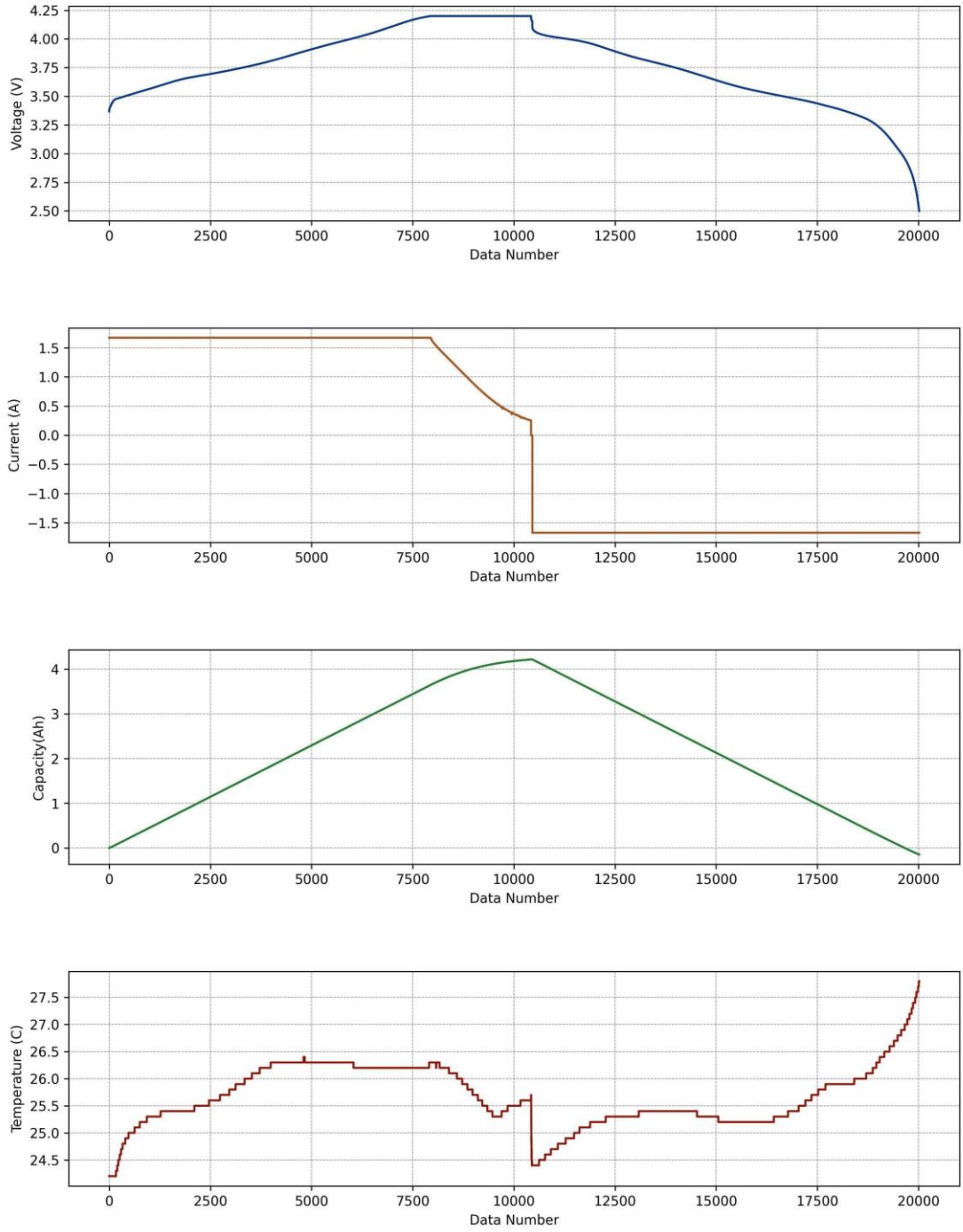

Figure 1. Dataset properties

The column data of the dataset used in this study is visualized in Figure 1. It is observed that the voltage value and capacity of the battery increase while charging with constant current, and the temperature value also increases. The dataset is rearranged to consist of four columns. The temperature column is the row estimated by the UKF method.

Chaos Particle Swarm Optimization

Both the quality of the solution and the PSO algorithm's rate of convergence depend on how the particle swarm is initialized. Since there is no previous information available, random initialization is often used to establish the position and velocity of the particles during the particle swarm initialization step. While particle swarms with random distributions are somewhat successful, certain particles may slow down the algorithm's convergence

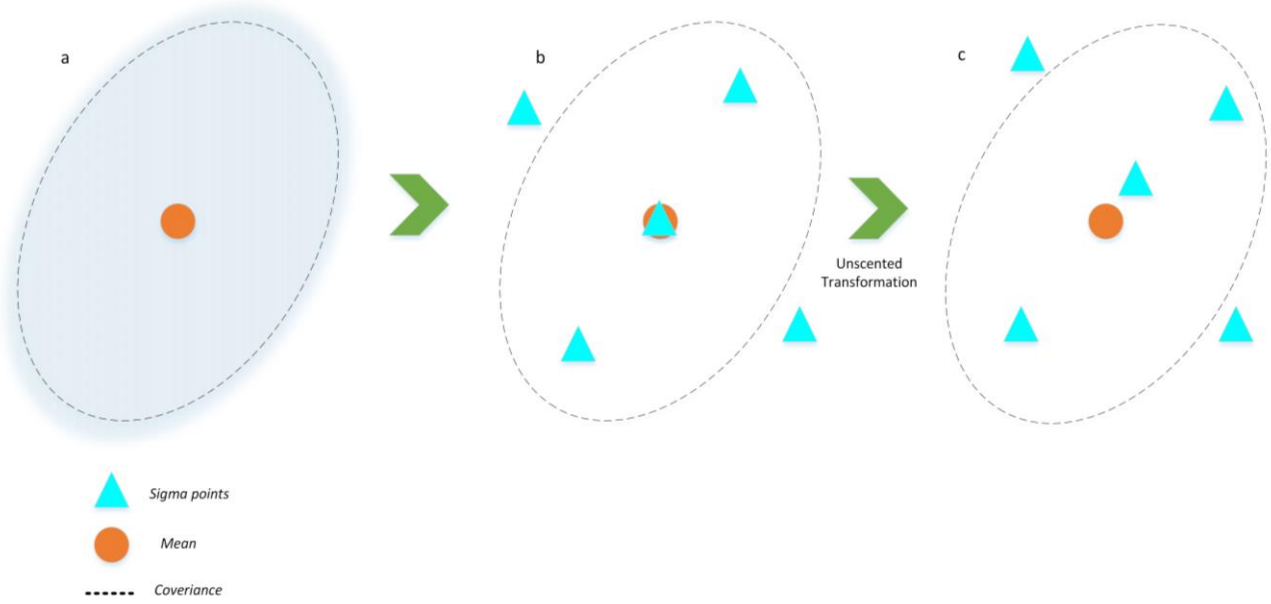

Figure 3. Unscented transformation

because they are too distant from the best answer. In the chaotic attraction domain, chaotic motion takes place in a variety of states while maintaining the necessary unpredictability of particle group initiation. A comparatively frequent occurrence in nonlinear systems is chaos. The law claims that it can traverse all states within a certain range and is ergodic and intrinsically random. Equation 2 presents the mapping relationship for a typical chaotic system, which is the logistic mapping [18].

$$z_{i+1} = \mu z_i(1 - z_i), z_i \epsilon (0,1] \quad (2)$$

In this case, the control variable is μ. The logistic map becomes fully chaotic at μ = 4, and the resultant chaotic variable zi exhibits superior ergodicity.

The logistic chaotic map's bifurcation diagram is seen in Figure 2.

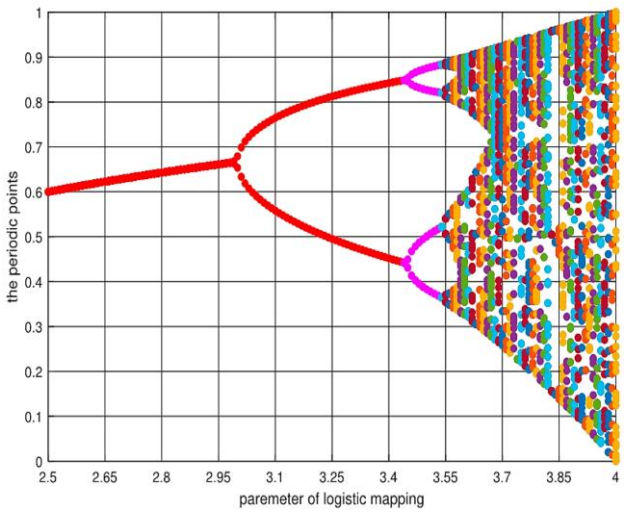

Figure 2. CPSO search [18]

During the search, the particle swarm can be distributed via the chaotic map to a random value in the interval [0, 1]. Nevertheless, as Figure 1 illustrates, the particles are more widely distributed in the region of 0 and 1 via the conventional chaotic mapping procedure in Equation 1. Because of this, the chaotic distribution is not uniform, which makes it impossible for the particles to be distributed evenly in the [0, 1] interval during the chaotic search process [18].

Unscented Kalman Filter

When used on a linear model, the Kalman filter is one specific kind of recursive Bayesian filter. For use with non-linear models, the extended Kalman filter (EKF) and unscented Kalman filter (UKF) are improvements over the Kalman filter. Although the UKF performs better in non-linear systems and small observed data regimes than the EKF, it should be emphasized that it is more computationally costly. Developed originally by Julier and Uhlman, the UKF is a flexible filter suitable for complicated non-linear systems. It makes use of the notion of unscented transformation to approximate the statistics of non-linear systems that are reasonably complicated. In the unscented transformation, a set of sample points is selected deterministically in order to mimic the statistical features of a random variable. It refers to these as sigma points. To perform the non-linear transformation, each sigma point is propagated across the non-linear systems. The statistical characteristics of the modified random variable are represented by these transformed sets of points [19]. Sigma points are used in the unscented transformation, as shown in Figure 3.

C represents the updated sigma points, *b* represents the production of symmetric sigma points around the mean, and *a* represents the a priori data.

KF theory is currently widely applied in various high-tech industries, including tracking, guiding, military applications, agriculture, and defense. A discrete linear time-varying system is given by Equation 3 and Equation 4.

$$x(k+1) = A(k)x(k) + B(k)u(k) + e(k) \tag{3}$$

$$y(k) = C(k)x(k) + \varepsilon(k) \tag{4}$$

The time step in this case is k, and the system status, control, and output variables are, respectively, $x \in R^n$, $b \in R^r$, and $y \in R^m$. Process noise (e) and measurement noise (ε) are uncorrelated and normally distributed zero-mean white noise sequences; Q and R are the variances of e and ε, respectively. A, B, and C are matrices with appropriate dimensions.

The UKF method based on unscented transformation (UT) was proposed by Julier [20]. UKF adheres to the KF structure; however, it expands and maps the Sigma point set in a nonlinear manner by projecting the state at the next moment. It has three benefits: first, it eliminates the need for the laborious computation of the complex nonlinear function's Jacobian matrix; second, it ensures the nonlinear system's universal adaptability; and third, the noise of the Gaussian distribution is reduced as a result of the Gaussian distribution's expanding Sigma point set. It specifies the UKF-based filtering procedure for the nonlinear time-varying system shown in Equation 5 and Equation 6.

$$x(k+1) = f\big(k, x(k), u(k)\big) + e(k) \tag{5}$$

$$y(k) = h\big(k, x(k)\big) + \varepsilon(k) \tag{6}$$

First, UT is used to determine the $2n$+1 Sigma sampling points and the weights that correlate to them. In this case, symmetric distribution sampling with UT is used. The situation is given in Equation 7.

$$X^{(i)}(k+1|k) = f\big[k, X^{(i)}(k|k), u(k)\big] \tag{7}$$

Then, the estimation results and covariance matrix of the system state variables are obtained as in Equation 8 and Equation 9.

$$\hat{X}(k+1|k) = \sum_{i=0}^{2n} w^{(i)} X^{(i)}(k+1|k) \tag{8}$$

$$P(k+1|k) = \sum_{i=0}^{2n} w^{(i)} \big[\hat{X}(k+1|k) - X^{(i)}(k+1|k)\big]\big[\hat{X}(k+1|k) - X^{(i)}(k+1|k)\big]^T + Q \tag{9}$$

To get *2n + 1* predicted observations *Y*, UT is used once more to construct a fresh set of Sigma points and accompanying weights based on the anticipated values. These values are then inserted into the nonlinear measurement function. This situation is given in Equation 10.

$$Y^{(i)}(k+1|k) = h\big[k, X^{(i)}(k+1|k)\big] \tag{10}$$

The update step is given in Equation 11, Equation 12 and Equation 13.

$$K(k+1) = P_{x_k y_k} P_{y_k y_k}^{-1} \tag{11}$$

$$\hat{x}(k+1|k+1) = \hat{X}(k+1|k) + K(k+1)[y(k+1) - \hat{Y}(k+1|k)] \tag{12}$$

$$P(k+1|k+1) = P(k+1|k) - K(k+1)P_{x_k y_k} K^T(k+1) \tag{13}$$

P is the variance, *k+1* is time, and *f(∗)* and *h(∗)* are the nonlinear function parameters [21]. The prediction metrics used in this study are given in Equation 22, Equation 23, Equation 24. Y is the true value, $\bar{y}$ is the mean of the true value and y_t^i is the predicted value [22].

$$MSE = \frac{1}{T}\sum_{t=1}^{T}(y - y_t^i)^2 \tag{14}$$

$$RMSE = \sqrt{\frac{1}{T}\sum_{t=1}^{T}(y - y_t^i)^2} \tag{15}$$

$$MAE = \frac{1}{T}\sum_{t=1}^{T}\left|y - y_t^i\right| \tag{16}$$

$$R^2 = \frac{\sum(y_t^i - y)^2}{\sum(\bar{y} - y)^2} \tag{17}$$

Results

It is critical that the temperature estimation of the lithium-ion battery is done by unscented Kalman filter-based methods. In this study, the hyperparameter values of the Unscented Kalman Filter Method are determined quickly by PSO and improved PSO methods, and then the battery temperature estimation is made. Table 2 shows the results found by PSO optimization and its derivatives for the sought parameter values of the UKF method in this study. The population number was determined as 50 for all optimization methods.

In Figure 4, the exploration and exploitation processes in the C-PSO method are presented graphically and the process of searching for a suitable solution in the optimization method is visualized. It is seen that the optimization method successfully achieved the stage of reaching a suitable solution by establishing a balanced search for the two concepts.

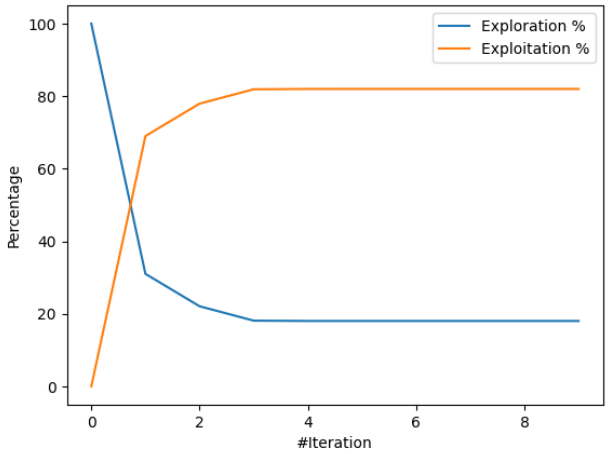

Figure 4. Hyperparameter search process of the CPSO-UKF method.

Table 3 shows the estimation success of the methods obtained by applying the hyperparameter values found by the optimization methods for the UKF method. When the lowest error was evaluated according to the MAE metric, the CPSO-UKF method made the least error with a value of 0.0000368. The UKF method was the method that made the most errors in prediction compared to the other methods. The PSO-UKF method made less error in

Table 2. Found hyperparameter by optimization method

	Alpha		Kappa		R	
Method	Search Area	Found	Search Area	Found	Search Area	Found
PSO	0.0001-0.1	0.0780940	0- 20	6.2504753	0.1-100	0.1006981
C-PSO	0.0001-0.1	0.0515949	0- 20	2.2726251	0.1-100	0.0000771
CL-PSO	0.0001-0.1	0.0656085	0- 20	19.0	0.1-100	0.2455204

Table 3. Estimation results of UKF methods

Method	MSE	RMSE	MAE	R^2
UKF	0.0172722	0.1314238	0.0012692	0.9463256
PSO-UKF	0.0000251	0.0050155	0.0000370	0.9999218
CPSO-UKF	0.0000248	0.0049817	0.0000368	**0.9999228**
CLPSO-UKF	0.0001376	0.0117342	0.0000871	0.9995721

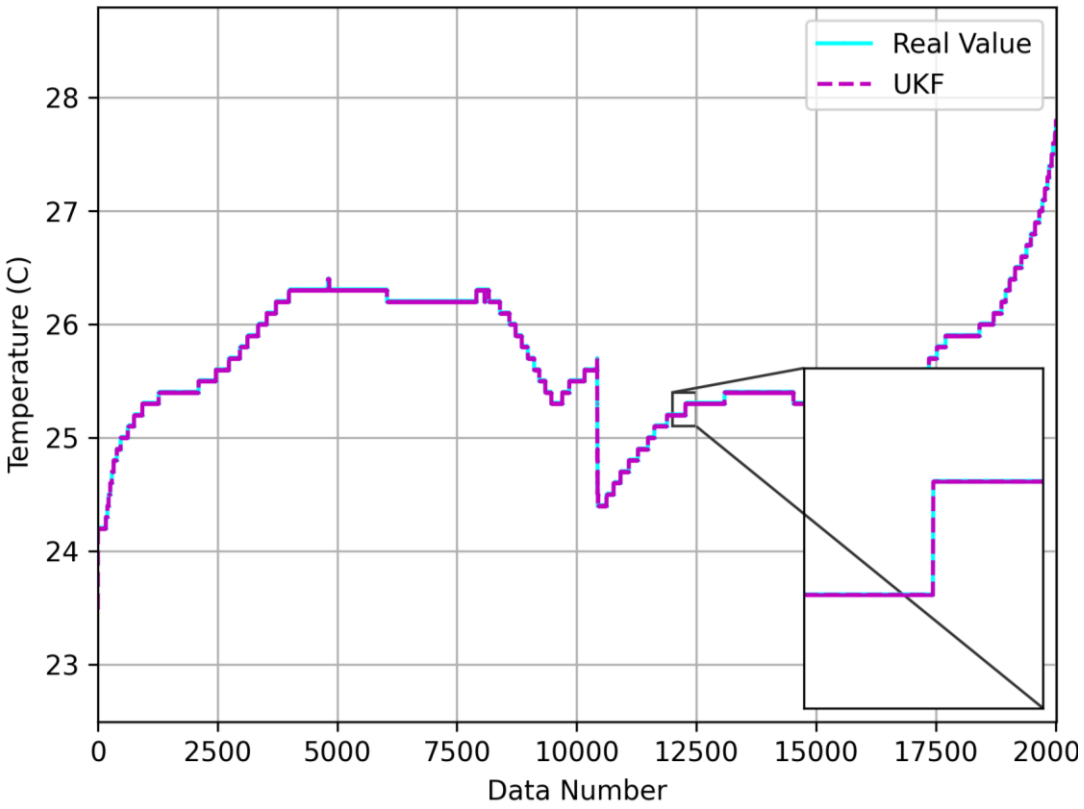

Figure 5. CPSO-UKF estimation result

prediction than the CLPSO-UKF method, with a value of 0.005013% according to the MAE metric. In Figure 5, a detailed comparison of the real value and the estimated values of the CPSO-UKF method is made. The CPSO-UKF method made a very small error in prediction from the real value with a value of 0.002482% according to the MSE metric. The temperature of the lithium-ion battery was successfully estimated using the Unscented Kalman Filter method.

All methods achieved more successful results than the normal UKF method. The CPSO -UKF method was the most successful method in temperature estimation with a value of 99.99228% according to the R^2 metric. The PSO-UKF method achieved more successful results than the standard UKF method. The CLPSO-UKF method achieved 0.03497% less success according to the R^2 metric than the PSO-UKF method.

Figure 5 provides the actual temperature value, and the temperature estimate by the using CPSO-UKF method. It is seen that the difference between the estimated value and the actual value is very small.

Conclusion

As the use of lithium-based batteries increases day by day, the improvement of energy consumption and performance of these batteries has become critical. In this study, temperature estimation of an 18650-type lithium-ion battery was made with UKF-based methods. Since the hyperparameter determination process is long and tiring, alpha, kappa, and R matrix values, which are among the most important hyperparameter values of the UKF method, were determined with PSO, CPSO, and CLPSO methods. In the hyperparameter search process, the population number was set as 50 for all optimization methods. By applying the obtained hyperparameter values to the UKF method, the lithium battery temperature estimation performances of the UKF, PSO-UKF, CPSO-UKF, and CLPSO-UKF methods were compared. All methods based on PSO optimization achieved more successful results compared to the standard UKF method. According to all experiments, the CPSO-UKF method was suggested as the most successful method with the least estimation error with a value of 0.49817% according to the RMSE metric. The process of finding the appropriate solution and the temperature estimation process of the proposed method were presented with different visuals and estimation metrics, and their success was presented. The author is considering using metaheuristic optimization methods in the lithium battery-based parameter estimation process with the particle filter method in future studies.

Ethics committee approval

There is no need to obtain permission from the ethics committee for the article prepared.

Conflict of Interest

There is no conflict of interest with any person / institution in the article prepared.

References

[1] M. Li, J. Lu, Z. Chen, and K. Amine, "30 Years of Lithium-Ion Batteries," Advanced Materials, vol. 30, no. 33, p. 1800561, 2018, doi: 10.1002/adma.201800561.

[2] B. Li et al., "A Review of Solid Electrolyte Interphase (SEI) and Dendrite Formation in Lithium Batteries," Electrochem. Energy Rev., vol. 6, no. 1, p. 7, Mar. 2023, doi: 10.1007/s41918-022-00147-5.

[3] X. Chen et al., "Practical Application of All-Solid-State Lithium Batteries Based on High-Voltage Cathodes: Challenges and Progress," Advanced Energy Materials, vol. 13, no. 35, p. 2301230, 2023, doi: 10.1002/aenm.202301230.

[4] S. M. Abu et al., "State of the art of lithium-ion battery material potentials: An analytical evaluations, issues and future research directions," Journal of Cleaner Production, vol. 394, p. 136246, Mar. 2023, doi: 10.1016/j.jclepro.2023.136246.

[5] A. Senyshyn, M. J. Mühlbauer, O. Dolotko, and H. Ehrenberg, "Low-temperature performance of Li-ion batteries: The behavior of lithiated graphite," Journal of Power Sources, vol. 282, pp. 235–240, May 2015, doi: 10.1016/j.jpowsour.2015.02.008.

[6] A. Belgibayeva et al., "Lithium-ion batteries for low-temperature applications: Limiting factors and solutions," Journal of Power Sources, vol. 557, p. 232550, Feb. 2023, doi: 10.1016/j.jpowsour.2022.232550.

[7] X. Su et al., "Liquid electrolytes for low-temperature lithium batteries: main limitations, current advances, and future perspectives," Energy Storage Materials, vol. 56, pp. 642–663, Feb. 2023, doi: 10.1016/j.ensm.2023.01.044.

[8] M. Waseem, M. Ahmad, A. Parveen, and M. Suhaib, "Battery technologies and functionality of battery management system for EVs: Current status, key challenges, and future prospectives," Journal of Power Sources, vol. 580, p. 233349, Oct. 2023, doi: 10.1016/j.jpowsour.2023.233349.

[9] R. R. Kumar, C. Bharatiraja, K. Udhayakumar, S. Devakirubakaran, K. S. Sekar, and L. Mihet-Popa, "Advances in Batteries, Battery Modeling, Battery Management System, Battery Thermal Management, SOC, SOH, and Charge/Discharge Characteristics in EV Applications," IEEE Access, vol. 11, pp. 105761–105809, 2023, doi: 10.1109/ACCESS.2023.3318121.

[10] G. Taş, C. Bal, and A. Uysal, "Performance comparison of lithium polymer battery SOC estimation using GWO-BiLSTM and cutting-edge deep learning methods," Electr Eng, vol. 105, no. 5, pp. 3383–3397, Oct. 2023, doi: 10.1007/s00202-023-01934-z.

[11] M. Zhang et al., "Electrochemical Impedance Spectroscopy: A New Chapter in the Fast and Accurate Estimation of the State of Health for Lithium-Ion Batteries," Energies, vol. 16, no. 4, Art. no. 4, Jan. 2023, doi: 10.3390/en16041599.

[12] B. Liu, X. Tang, and F. Gao, "Joint estimation of battery state-of-charge and state-of-health based on a simplified pseudo-two-dimensional model," Electrochimica Acta, vol. 344, p. 136098, Jun. 2020, doi: 10.1016/j.electacta.2020.136098.

[13] J. Qiao, S. Wang, C. Yu, X. Yang, and C. Fernandez, "A chaotic firefly - Particle filtering method of dynamic migration modeling for the state-of-charge and state-of-health co-estimation of a lithium-ion battery performance," Energy, vol. 263, p. 126164, Jan. 2023, doi: 10.1016/j.energy.2022.126164.

[14] C. Wang, S. Wang, J. Zhou, J. Qiao, X. Yang, and Y. Xie, "A novel back propagation neural network-dual extended Kalman filter method for state-of-charge and state-of-health co-estimation of lithium-ion batteries based on limited memory least square algorithm," Journal of Energy Storage, vol. 59, p. 106563, Mar. 2023, doi: 10.1016/j.est.2022.106563.

[15] W. Li, M. Rentemeister, J. Badeda, D. Jöst, D. Schulte, and D. U. Sauer, "Digital twin for battery systems: Cloud battery management system with online state-of-charge and state-of-health estimation," Journal of Energy Storage, vol. 30, p. 101557, Aug. 2020, doi: 10.1016/j.est.2020.101557.

[16] M. Rashid, M. Faraji-Niri, J. Sansom, M. Sheikh, D. Widanage, and J. Marco, "Dataset for rapid state of health estimation of lithium batteries using EIS and machine learning: Training and validation," Data in Brief, vol. 48, p. 109157, Jun. 2023, doi: 10.1016/j.dib.2023.109157.

[17] DNKPOWER, "3.63V-4850mAh-18.20Wh-LG-M50-21700 Battery," Lithium ion Battery Manufacturer and Supplier in China-DNK Power. Accessed: Aug. 03, 2024. [Online]. Available: https://www.dnkpower.com/lg-m5021700-m50t21700/

[18] Z. Ma, X. Yuan, S. Han, D. Sun, and Y. Ma, "Improved Chaotic Particle Swarm Optimization Algorithm with More Symmetric Distribution for Numerical Function Optimization," Symmetry, vol. 11, no. 7, Art. no. 7, Jul. 2019, doi: 10.3390/sym11070876.

[19] N. M. M. Kalimullah, K. Shukla, A. Shelke, and A. Habib, "Stiffness tensor estimation of anisotropic crystal using point contact method and unscented Kalman filter," Ultrasonics, vol. 131, p. 106939, May 2023, doi: 10.1016/j.ultras.2023.106939.

[20] J. Shen et al., "Alternative combined co-estimation of state of charge and capacity for lithium-ion batteries in wide temperature scope," Energy, vol. 244, p. 123236, Apr. 2022, doi: 10.1016/j.energy.2022.123236.

[21] Z. Long, M. Bai, M. Ren, J. Liu, and D. Yu, "Fault detection and isolation of aeroengine combustion chamber based on unscented Kalman filter method fusing artificial neural network," Energy, vol. 272, p. 127068, Jun. 2023, doi: 10.1016/j.energy.2023.127068.

[22] G. Taş, A. Uysal, and C. Bal, "A New Lithium Polymer Battery Dataset with Different Discharge Levels: SOC Estimation of Lithium Polymer Batteries with Different Convolutional Neural Network Models," Arab J Sci Eng, vol. 48, no. 5, pp. 6873–6888, May 2023, doi: 10.1007/s13369-022-07586-8.